Low-frequency seismic properties of olivine-orthopyroxene mixtures

Tongzhang Qu[1], Ian Jackson[1], Ulrich H. Faul[1,2]
1 Research School of Earth Sciences, Australian National University, Canberra, Australia
2 Earth Atmospheric and Planetary Sciences, Massachusetts Institute of Technology, Cambridge, MA, USA

Introduction

Seismological structures are the manifest of combined influence from temperature, parital melting etc. Variation of seismic properties (e.g. modulus or dissipation) with each of the factors could help interpret seismological structures.

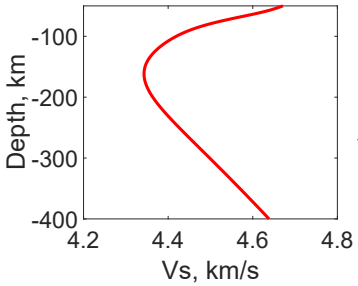

seismic properties

- temperature
- melt
- phase transition
- grain size
- water
- redox conditions
- etc.

Low-frequency seismic properties of olivine-orthopyroxene mixtures

Relative to high-frequency measurement where the applied stress is at kHz – GHz, low-frequency measurement at mHz – Hz allows time for relaxation at high temperature.

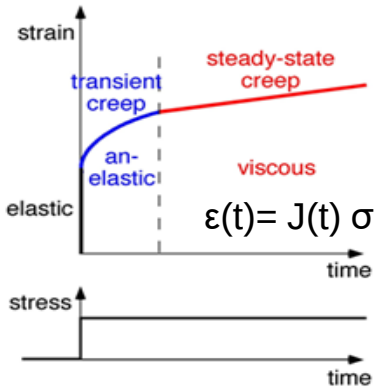

Olivine: the most abundant mineral in the upper mantle
– whose seismic properties are well studied.

Orthopyroxene: the 2nd most abundant mineral in the upper mantle, up to 30%
– whose seismic properties received less attention.

In this study, two synthetic specimens of $Ol_{70}Opx_{30}$ and Ol_5Opx_{95} composition were mechanically tested by torsional forced oscillation at elevated temperatures under confining pressure of 200 MPa.

Experimental methods

1) Sample preparation: sol-gel polycrystalline olivine and orthopyroxene mixtures

Tested specimens
1755: $Ol_{70}Opx_{30}$
1777: Ol_5Opx_{95}
1842: Ol_5Opx_{95}, recycled 1777
(Ol = Fo_{90}, Opx = En_{90})

Expected phase transition at temperature > 1000°C
Orthopyroxene (Pbca) ↔ Protopyroxene (Pbcn)

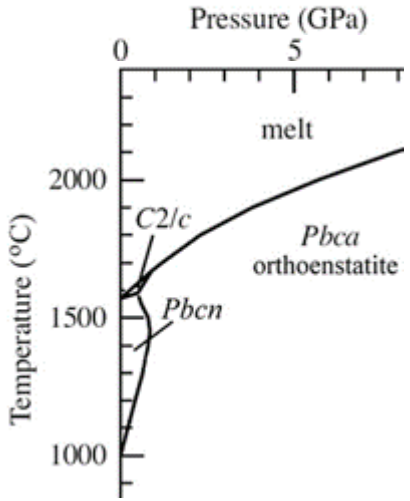

Fig.1 Phase diagram of enstatite (after Presnall, 1995). Low Fe content does not notably affect the boundary of phase.

2) Torsional forced oscillation testing

Oscillation frequencies: Hz – mHz

Temperature: 1300/1200 °C – 400 °C

Confining pressure: 200 MPa

Strain < 10^{-5}

In short, same torque is applied to the specimen and the elastic standard. Shear modulus and dissipation of the specimen are measured by comparison between the specimen strain and elastic standard strain.

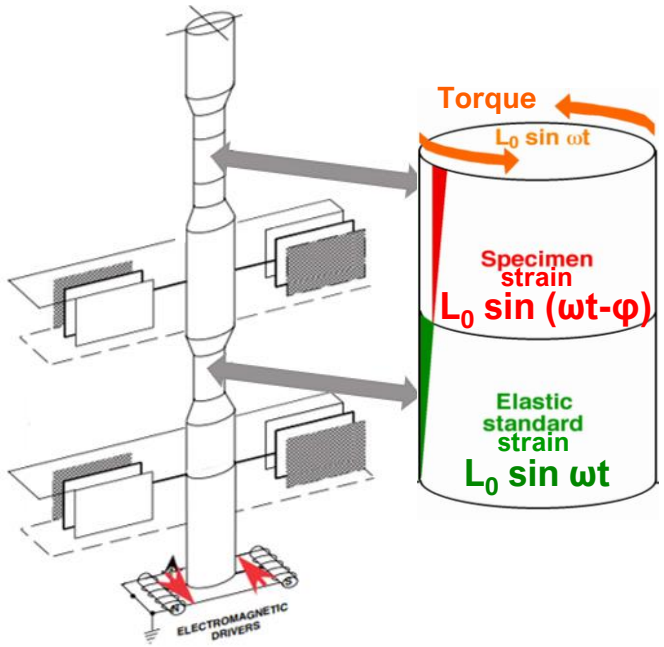

Fig.2 Schematic diagram of torsional forced oscillation. The phase lag φ in specimen strain is the manifest of viscoelastic relaxation.

3) Extended Burgers model

The data pairs (G, Q^{-1}) for temperatures ≳ 900ºC and $\log_{10}Q^{-1}$ ≳ -2.2 were fitted by a model based on an extended Burgers-type creep function,

$$J(t) = J_U\left\{1 + \Delta\int_0^\infty D(\tau)\left[1 - exp\left(\frac{-t}{\tau}\right)\right]d\tau + \frac{t}{\tau_M}\right\}$$

with separately normalized distributions of anelastic relaxation time (Barnhoorn et al., 2016). In this way, the data could be parameterized for further analysis.

Characterization of samples

1) Grain size, density and chemical composition

Specimen	d, μm	ρ, g/cm^3		SiO_2 wt.%	FeO wt.%	MgO wt.%	Mg#
1755 $Ol_{70}Opx_{30}$	< 2.7	3.28	Ol	40.7	10.8	48.7	88.9
			Opx	58.0	6.8	35.7	90.4
1777 Ol_5Opx_{95}	< 2.4	3.16	Ol	41.8	11.4	48.1	88.3
			Opx	58.3	7.1	35.3	89.9
1842 Ol_5Opx_{95}	< 3.0	NA	Ol	43.9	11.0	46.1	88.2
			Opx	57.4	7.2	35.3	89.8

2) Microstructures after mechanical testing

For all the BSE images lighter phase is olivine, and darker phase is orthopyroxene.

1755 $Ol_{70}Opx_{30}$

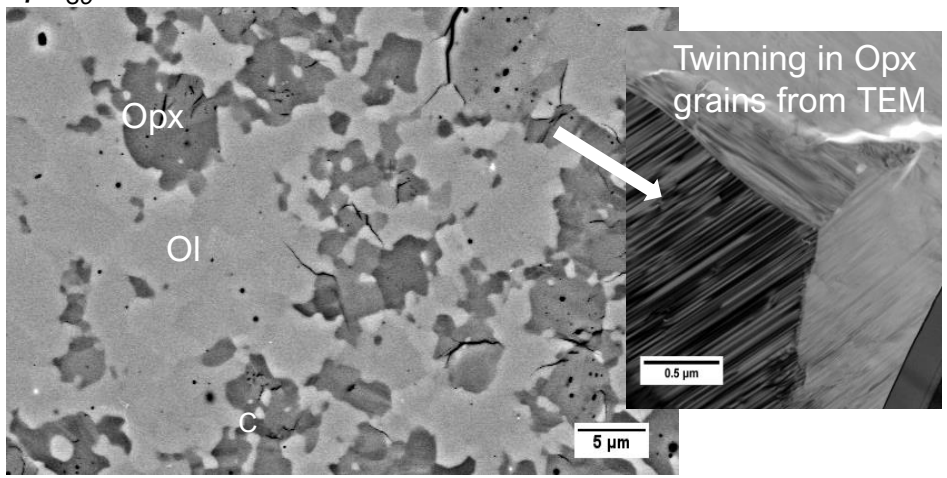

Fig.3 BSE and TEM images of 1755.

1777 Ol_5Opx_{95}

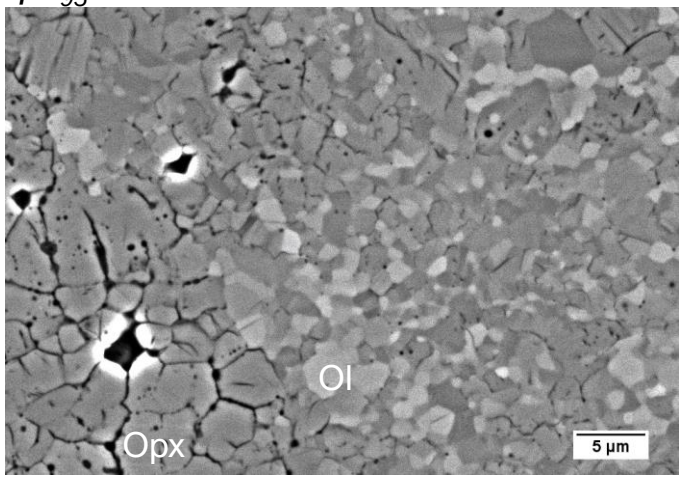

Fig.4 SEM-BSE image of specimen 1777.

1842 Ol_5Opx_{95}, recycled 1777

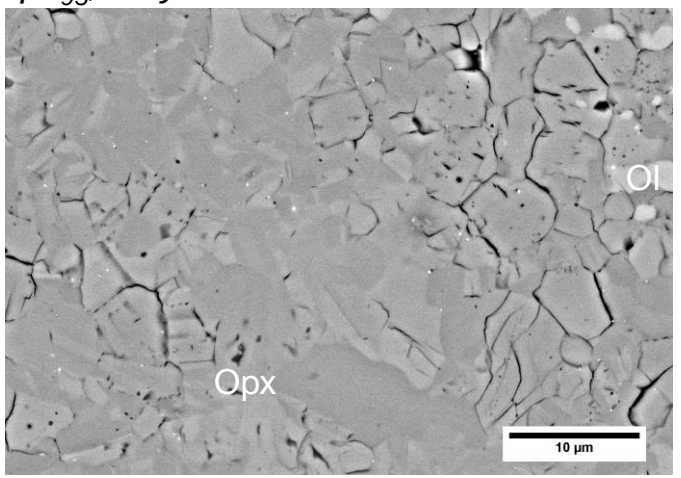

Fig.5 BSE image of specimen 1842, recycled 1777.

Results

Forced-oscillation data: shear modulus (G) and dissipation (Q^{-1}) at various temperature in mHz – Hz domain at high temperature

As the manifest of viscoelastic relaxation, the dynamic shear modulus and dissipation vary monotonically with temperature and frequency.

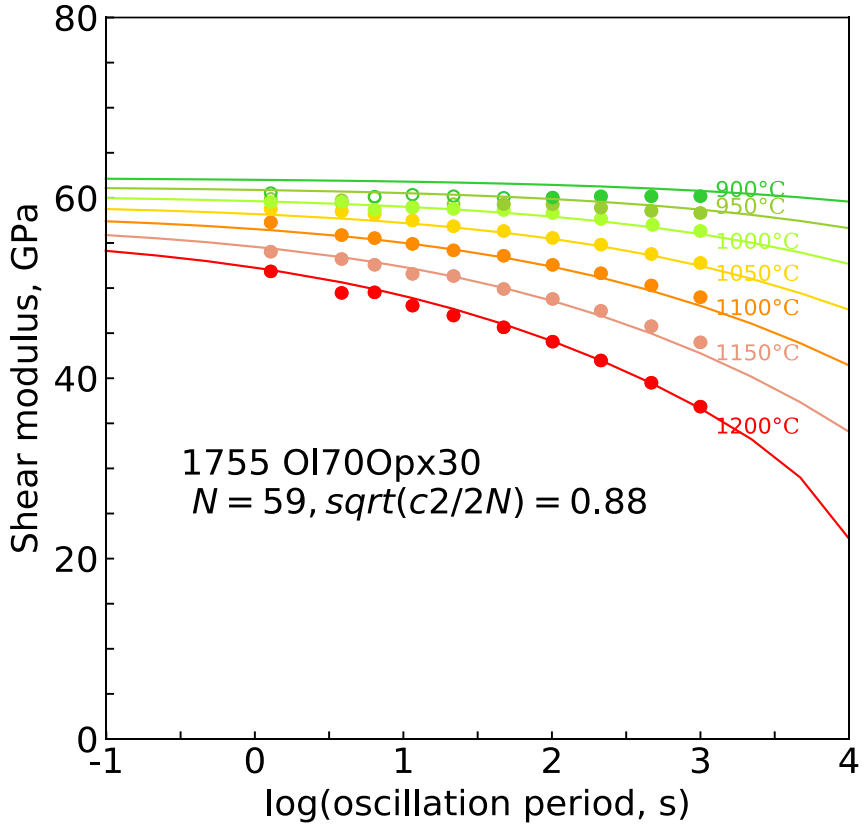

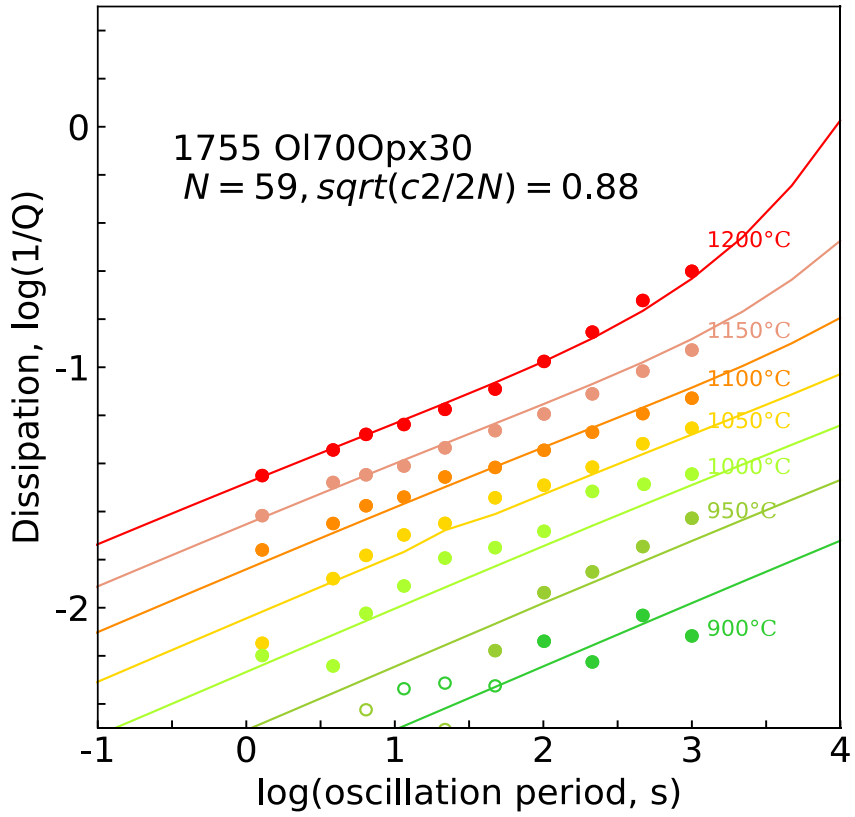

Results

1) The results of 1755 ($Ol_{70}Opx_{30}$) and run 1127 ($Ol_{95}Opx_{5}$) look overall very similar in terms of frequency and temperature dependence. Note that 30% is about the maximum Opx content in the Earth' s upper mantle.

   Some experimental setup of run 1127 is different from testing with opx-rich specimens in this study. We are going to run a follow-up testing with $Ol_{95}Opx_{5}$ specimen with modern experimental setup.

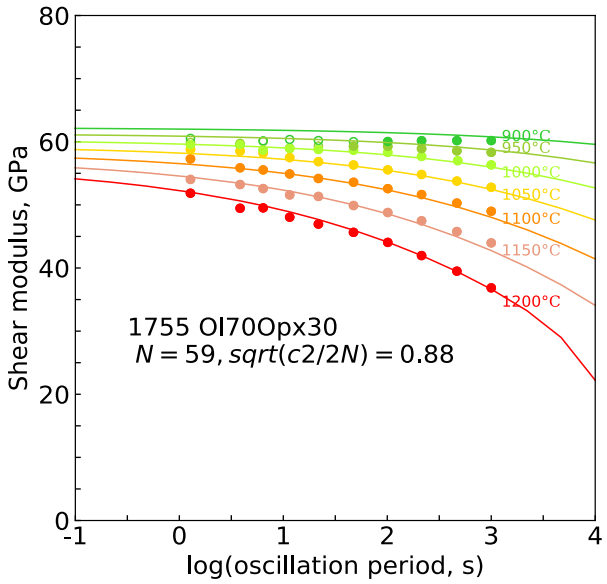

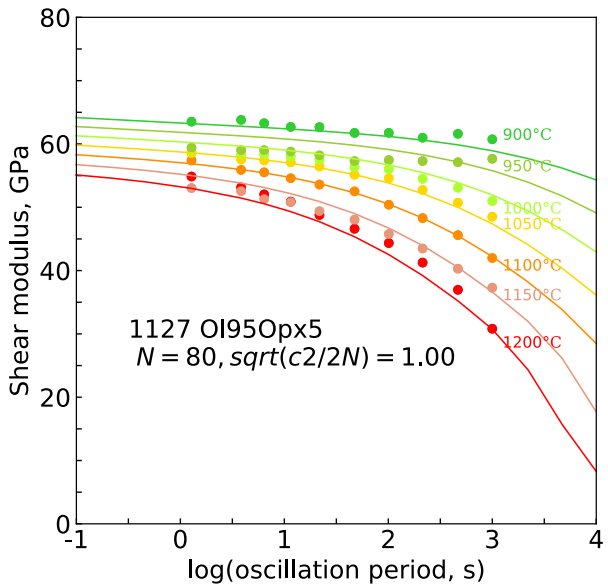

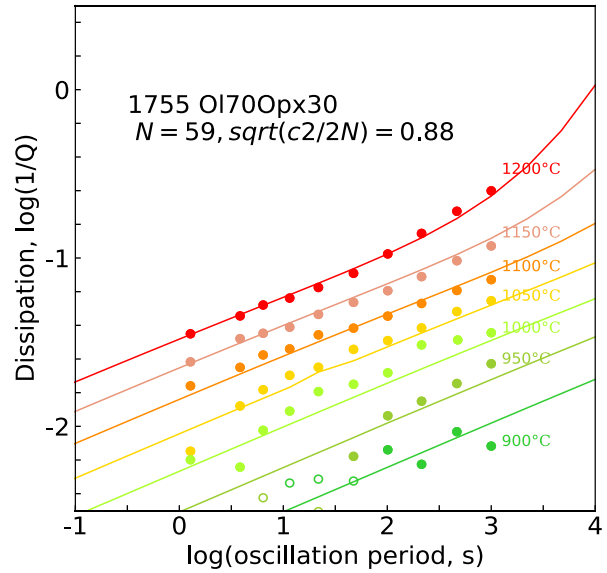

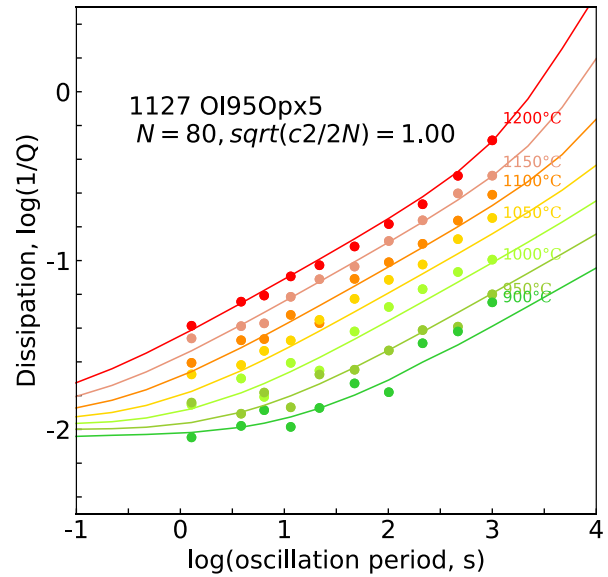

Results

2) One Burgers model cannot fit the data across all the temperatures. The Ol_5Opx_{95} specimen (recycled 1777) in 1842 is anomalously dispersive and dissipative at the highest temperatures of 1300 and 1275 °C. Accordingly, these data have been excluded from the fitted dataset. This may reflect ortho-proto phase transition.

In previous run 1127 (Opx5), 1755 (Opx30) and 1777 (Opx95) where the temperature cooled from 1200 °C, the data could be fitted with one Burgers model for each measurement.

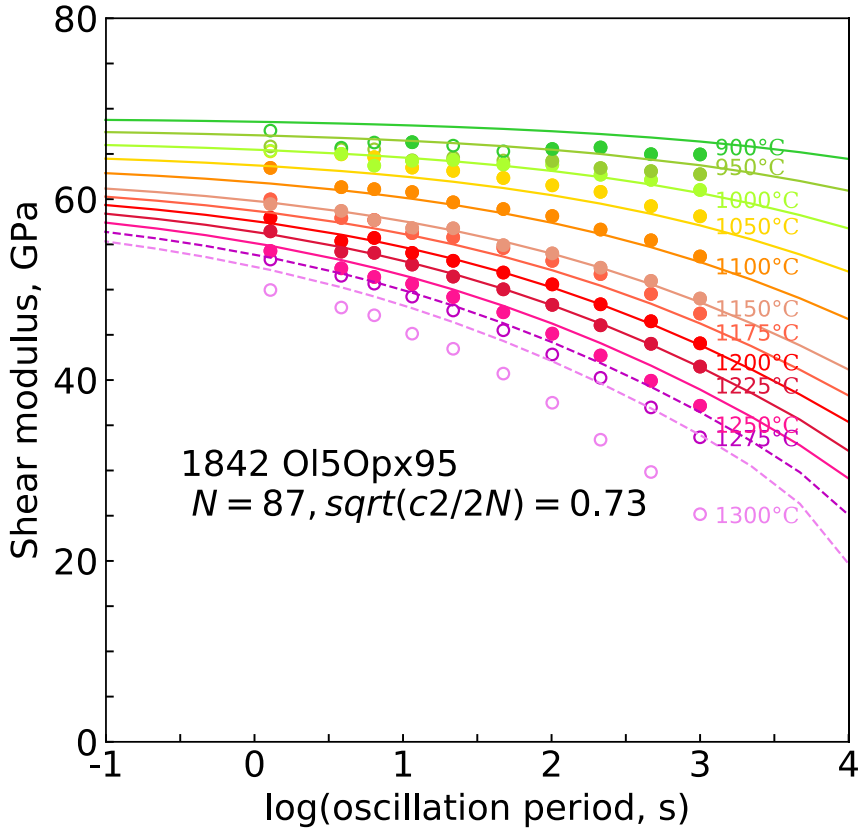

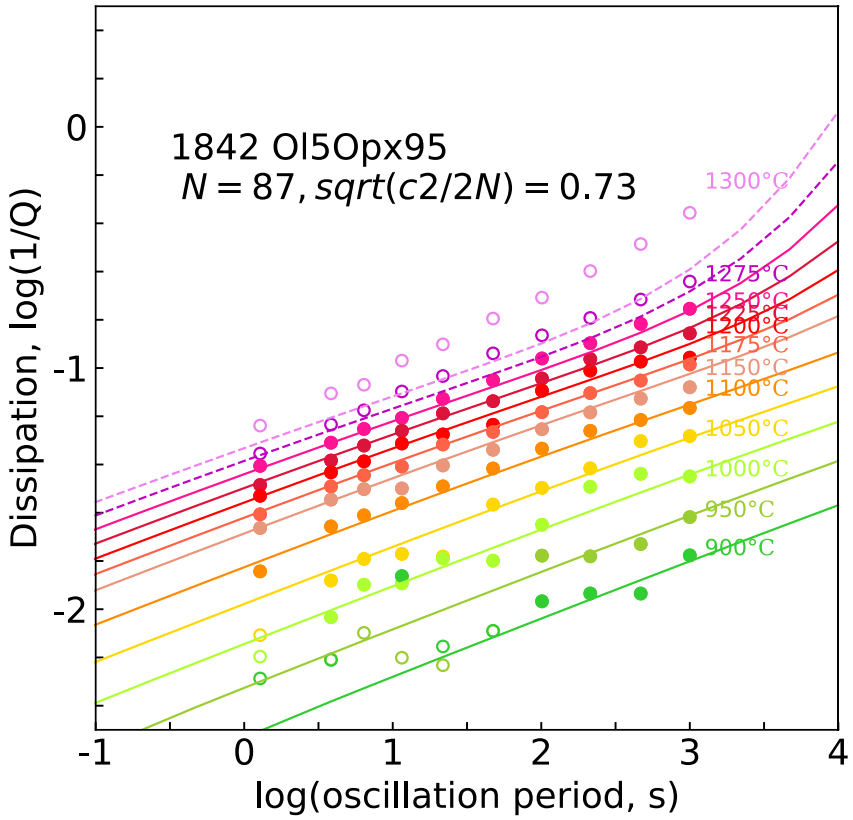

Discussion

1) Influence of increasing Opx content

The higher orthopyroxene concentrations are associated with systematically somewhat lower levels of dissipation and corresponding weaker modulus dispersion at 1200 °C. Below 1200 °C, the dissipation level is similar.

1755
Sol-gel $Ol_{70}Opx_{30}$, melt-free, d < 2.7 µm

1842
Sol-gel Ol_5Opx_{95}, melt-free, d ~ 3 µm

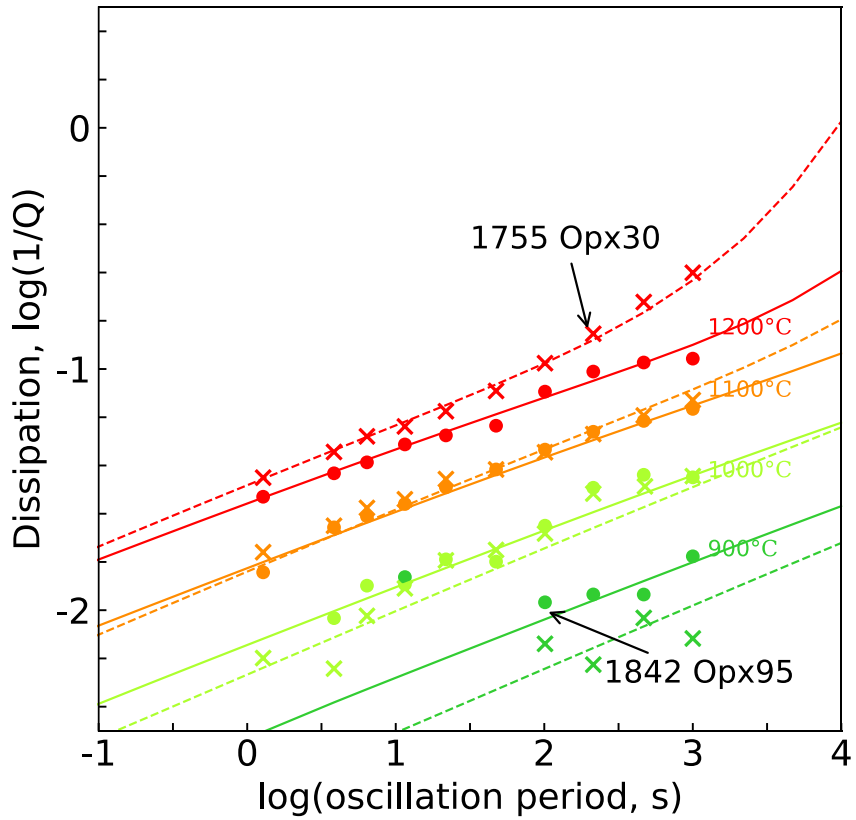

Discussion

2) Similar Opx content but different annealing temperature

The sample specimen was tested from 1200 °C in 1777 (Opx95) and 1300 °C in 1842 (Opx95, recycled 1777). The modulus dispersion and dissipation for the specimen remain similar through the two tests. This confirms the reproductivity of our inelastic property measurement.

The main difference is again at 1200 °C, similar to the comparison between 1755 (Opx30) and 1842 (Opx95). This further indicates that there is some notable mechanical influence from proto-ortho phase transition above 1200 °C.

1777: sol-gel Ol_5Opx_{95}, melt-free, d < 2.7 μm
1842: sol-gel Ol_5Opx_{95}, melt-free, d ~ 3 μm, recycled 1777

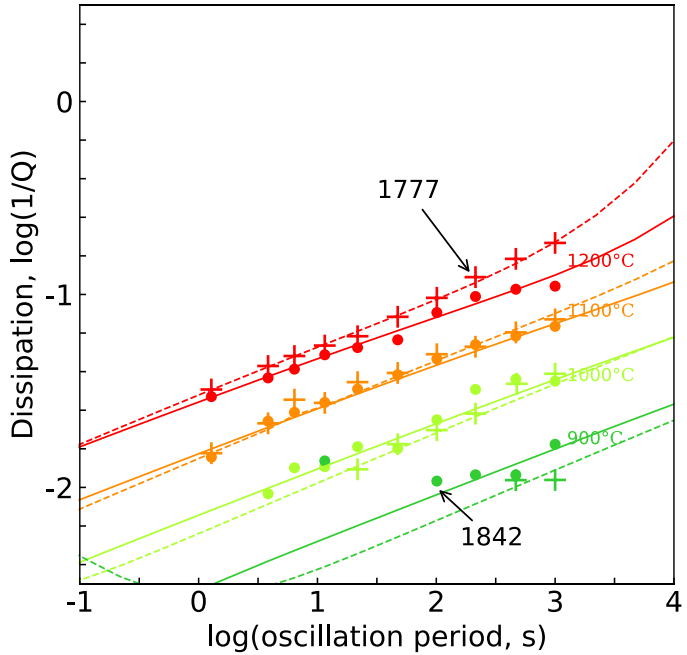

Discussion

3) Similar Opx content but different melt fraction

Systematically much higher modulus and lower dissipation for the melt-free material of the present study.

No evidence of dissipation peak reported by Sundberg and Cooper (2010) for an $Ol_{60}Opx_{40}$ specimen prepared from natural precursor materials with ~1.5% melt content.

1755: sol-gel $Ol_{70}Opx_{30}$, melt-free, d < 2.7 µm
Sundberg & Cooper (2010): natural-precursor $Ol_{60}Opx_{40}$ with 1.5% melt, d ~ 5.2 µm

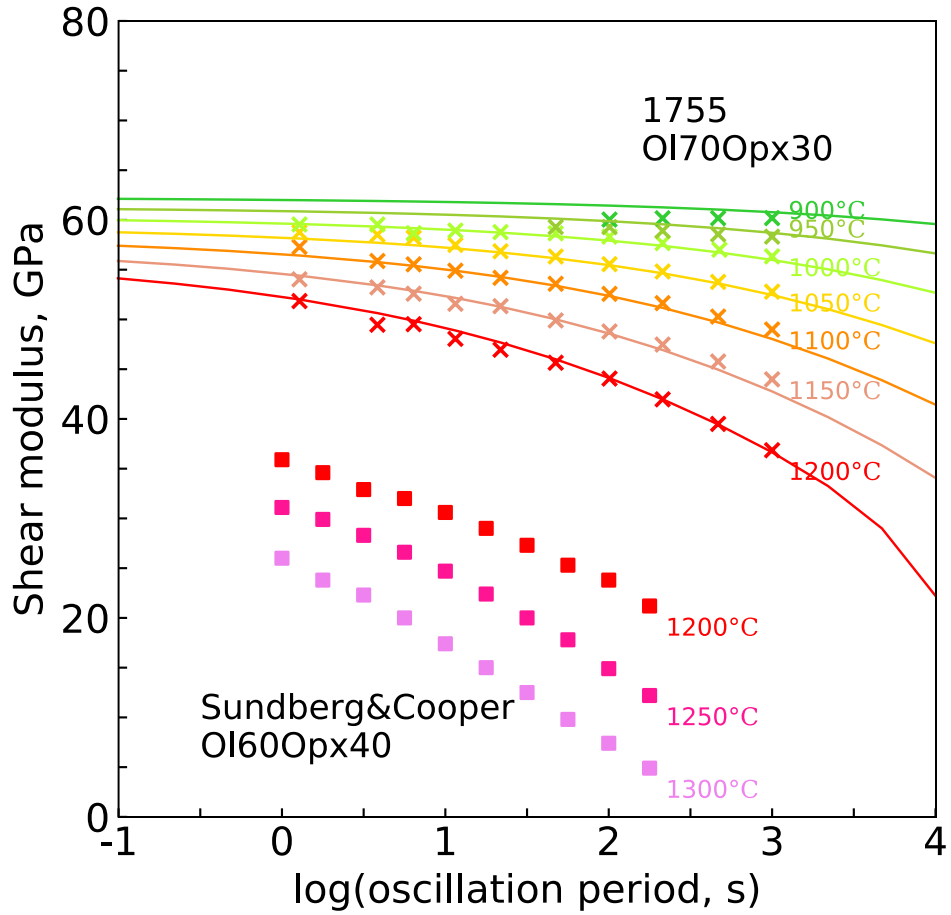

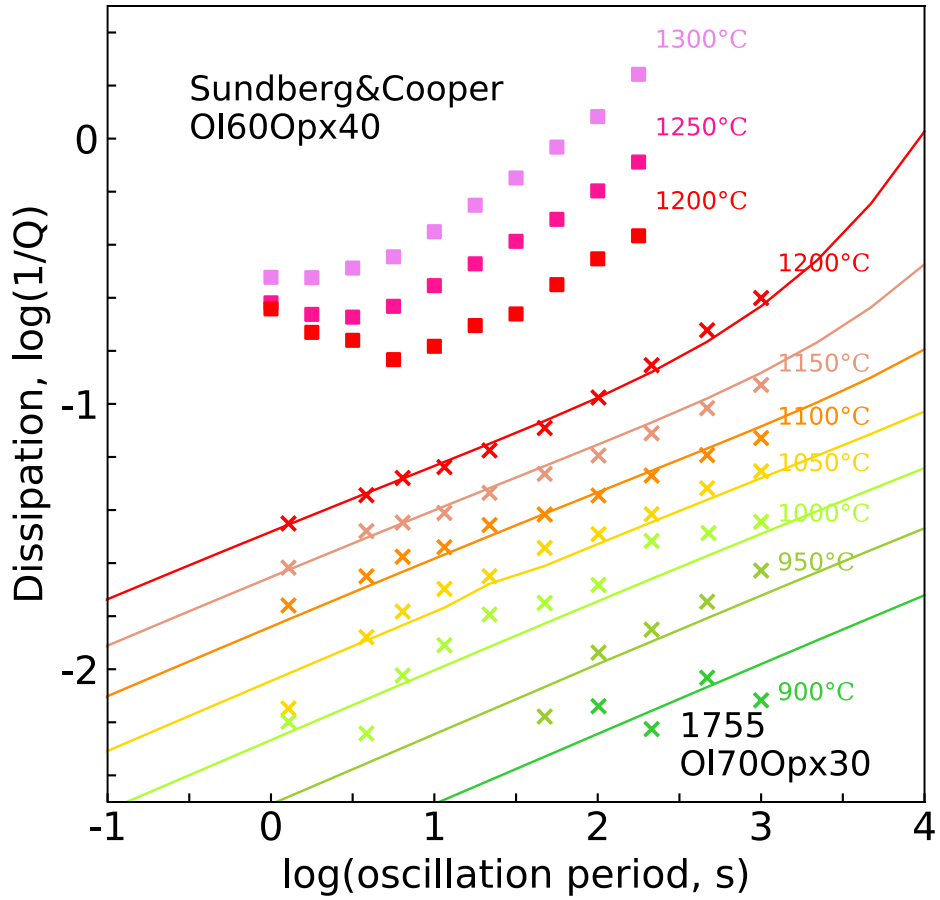

Conclusions

1) The viscoelastic behaviour is high-temperature-background type without any evidence of the superimposed dissipation peak reported by Sundberg and Cooper (2010) for a melt-bearing specimen of otherwise similar composition.

2) The proto-to-ortho pyroxene phase transition is reflected by the discontinuity of mechanical behaviour near 1250 ºC.

3) Dissipation level and its frequency dependence, and modulus dispersion are overall similar but somewhat diminished and slightly more temperature-sensitive with higher Opx concentration - to be confirmed by another testing on pure sol-gel olivine specimen.

4) The olivine-based model for high-temperature viscoelasticity or attenuation model will require only modest modification to accommodate the role of orthopyroxene.